Optimized Active Cooling and Refrigeration using Antidotted Graphene for Heat Management of Microelectronics

Shuang Tang,* Andy Juan, David Drysdale, Joseph Duarte Menjivar and Jason Guzman

Abstract

With the technology of artificial defects creating, we can tune the band structure and transport properties of many two-dimensional (2D) layered materials. One prototype materials system is the antidotted graphene sheet, where periodical pores are made using focused ion or electron beams in the nanoscale. Here, we study the electrical conductivity, thermopower, and active rates of cooling and refrigeration of antidotted graphene samples with different pore-radii and interporous distances. We use a calculation method that takes into consideration the sensitivity of transport to charge carrier energy, which can be used to describe the elastic and inelastic scatterings in diffusive, ballistic, and quantum hopping regimes. It is found that our results from the new calculational approach are more consistent with the experimental data compared to some traditional methodologies. It is also interesting to see that the optimized active rates of cooling and refrigeration are very robust against the distribution variations of interporous distance and the pore-radius, which implies easy industrialization and inexpensive manufacturing. The same analysis and investigation can also be extended to many other layered materials, including transitional metal dichalcogenides (TMD), blue phosphorene, and tellurene.

1. Introduction

As we are reaching the limit of Moore's law[1] in upgrading computer chips based on the silicon materials system, many new candidates have been proposed for the next generation of microelectronics, including graphene,[2] blue phosphorene,[3] tellurene,[4] and other low-dimensional materials.[5,6] Besides the power consumption and computational frequency, the heat management of such microsystems is also an important issue that needs to be resolved. Beyond the micro-fluid systems for passive heat management, researchers have been interested in solid-state thermoelectric cooling and refrigeration technology,[7] which is non-noisy, non-fluid, compact, and easy to cascade. Many materials have been suggested to make thermoelectric cooling/refrigeration systems, including bismuth antimony thin films,[8-10] silicon-germanium nanowires,[11,12] lead telluride nanocomposites,[13,14] and others,[15] among which the graphene-based derivatives are attracting intensive interests,[16-18] which can be easily compacted with other layered materials of novel electronics. Antidotted graphene[19-24] are nanoporous materials that can be used to tune the band structure, the scattering mechanism, and thus, the transport properties of pristine graphene. Nanoscale pores can be made on a graphene layer using extreme ultraviolet light,[25,26] focused ion beam,[27,28] or electron beam lithography,[29,30] periodically or randomly. This subtractive process of pores introducing is referred to as antidoting. Xu *et al.*[30] has realized a thermopower of 26.3 μW/cm·K^2 at room temperature and 3.01 μW/cm·K^2 at the cryogenic temperature of 82 K, before optimization. Unfortunately, there is not a more detailed study on the optimized performance in active cooling and refrigeration using antidotted graphene sheets at both room and cryogenic temperatures.

The calculation of active cooling and refrigeration rates largely depends on the electrical conductivity and the thermopower. Many methodologies have been proposed and utilized in the calculation of electrical conductivity and thermopower for graphene and other materials systems, among which the semi-classical Boltzmann transport theory using the code of *BoltzTrap* code[31] and the maximally localized Wannier function method using the package of *Electron-Phonon Wannier* (*EPW*)[32] package are with special importance. The former is simplifying the calculation using a constant relaxation time approximation, and the latter is neglecting scatterings from mechanisms other than the

College of Engineering, State University of New York Polytechnic Institute, Albany, NY, 12203, USA
E-mail: tangs1@sunypoly.edu (S. Tang)

electron-phonon interaction. However, as Tang *et al*.[30,33,34] pointed out, the optimal thermopower is highly dependent on the specific carrier scattering mechanism(s), and hence the sensitivity of transport/scattering rate to the carrier energy. Therefore, a further advanced method should be employed to consider the influence of such energy sensitivity on the optimal thermopower, and thus, the active cooling and refrigeration rates.

In this paper, we will study the conductivity and thermopower by taking the carrier scattering mechanism-induced energy sensitivity into consideration with comparison to the *BoltzTrap* method,[31] the *EPW* method,[32] and the experimental data.[30] The active cooling and refrigeration rates of antidotted graphene sheets with different pore-radii and interpore distances will be then studied for both the room and the cryogenic temperatures.

2. Method

The electrical conductivity and the thermopower can be generally calculated as[33],

$$\sigma = q^2 \sum_{Bands} \int q\theta \left(-\frac{\partial f}{\partial E}\right) dE, \tag{1}$$

and

$$S = -\frac{k_B}{q} \frac{\sum_{Bands} \int q\theta\left(-\frac{\partial f}{\partial E}\right)\left(\frac{E-E_f}{k_BT}\right)dE}{\sum_{Bands} \int q\theta\left(-\frac{\partial f}{\partial E}\right)dE}, \tag{2}$$

where k_B is the Boltzmann constant, q is the positive or negative elementary charge, f is the probability distribution function of electrons and E_f is the Fermi level. The transport rate θ measures the density of free charge carriers passing across a unit area per unit of time and can be determined using an iterative approach[35-40] to consider both elastic and inelastic scatterings in diffusive,[41-44] ballistic[45-49] and quantum hopping transport regimes,[50-53] as

$$f(\boldsymbol{k}) = f_0[\varepsilon(\boldsymbol{k})] + x\theta(\boldsymbol{k}), \tag{3}$$

where $\boldsymbol{k}$ is the lattice momentum, f_0 is the *f* function when the system reaches an equilibrium, and x is the angle between the momentum $\boldsymbol{k}$ and the externally exerted force. The perturbation $\theta(\boldsymbol{k})$ can be updated iteratively by:

$$\theta(k) =$$
$$\frac{\chi_{i,in}[\theta(k)]+\chi_{e,in}[\theta(k)]+\chi_{b,in}[\theta(k)]+\chi_{h,in}[\theta(k)]-v(k)\left(\frac{\partial f}{\partial z}\right)-\frac{e\varepsilon}{\hbar}\nabla_k f}{\chi_{i,out}(k)+\chi_{e,out}(k)+\chi_{b,out}(k)+\chi_{h,out}(k)}, \tag{4}$$

where the $\chi_{in,*}$ and $\chi_{out,*}$ terms are counting the probability increment caused by inward and outward transport, respectively. The subscripts of "*i*", "*e*", "*b*", and "*h*" stand for inelastic, elastic, ballistic, and hopping scatterings/transports, respectively. The term $\left(\frac{\partial f}{\partial z}\right)$ is counting the change of probability density caused by the temperature gradient along the z direction, and the term $\frac{e\varepsilon}{\hbar}\nabla_k f$ is counting the effect of external electrical fields.

Tang *et al*.[30,33,34] has found that the energy sensitivity of carrier transport (*s*), which is representing the relative change of transport rate per unit relative change of carrier energy (ε) counting from the corresponding band edge $s = (d\theta/\theta)/(d\varepsilon/\varepsilon)$,

is a key factor that ultimately determines the optimal value of the thermopower during the integration of Eqs. (1) and (2), which are neglected in the *BoltzTrap* method[31] and the *EPW*[32] method. The value of such an energy sensitivity is determined by the specific materials system, the carrier scattering mechanisms, and the temperature.

Zebarjadi *et al*.[54] have pointed out that besides the passive thermal conductivity, the active cooling rate of a material caused by the thermoelectric effect can be calculated by

$$r_{a,c} = \frac{\sigma S^2 T_H}{2\Delta T}, \tag{5}$$

where T_C and T_H are the cold-side and hot-side temperatures, respectively, and $\Delta T = T_H - T_C$ is the temperature drop. The active refrigeration rate can, instead, be calculated by

$$r_{a,r} = \frac{\sigma S^2 T_c}{2\Delta T}. \tag{6}$$

The transport property of an antidotted graphene may be influenced by the shape of the pores, the pore-radius, and the interpore distance. Without loss of generality, we study the graphene samples antidotted with square pores, with different pore-radii and interpore distances as defined and illustrated in Fig. 1.

3. Results and discussions

From our previous study, we found that the energy sensitivity in squarely antidotted graphene is $s = 1.11$ for the room temperature of 300 K and $s = 0.30$ for the cryogenic temperature of 82 K.[30] The calculated thermopower of the antidotted graphene sample shown in Fig. 1(a) using our method is exhibited in Fig. 2, compared to the other two traditional methods. The comparison is suggesting that although using the constant relaxation time approximation or using the phonon scattering approximation can capture the main trend of the thermopower in a large range, our method can better capture the details near the maximum-value range, due to the incorporation of the information on energy sensitivity. In this case, the actual energy sensitivity in the antidotted graphene sample is larger than ~0 as assumed in the *BoltzTrap* method, and ~0.5 as assumed in the *EPW* method, which results in their underestimation of the optimal thermopower.

We then use our method to calculate the values of thermopower and power factor that are optimized against the gate voltage or Fermi level, for the four different antidoting cases shown in Fig. 1. As we can see from Fig. 3, the optimal values of thermopower differ noticeably in the four different samples. Since we can view the antidotted graphene as a network of nanoribbons, the width of the non-dotted ribbons regions will decide the confinement effect for the electrons and holes. Generally, the smaller the width is, the stronger the confinement effect we have and the larger mini-bandgap will be introduced to the graphene sample. Further, an increased mini-bandgap indicates a reduced bipolar effect that is causing a cancellation between the hole- and the electron-thermopower.
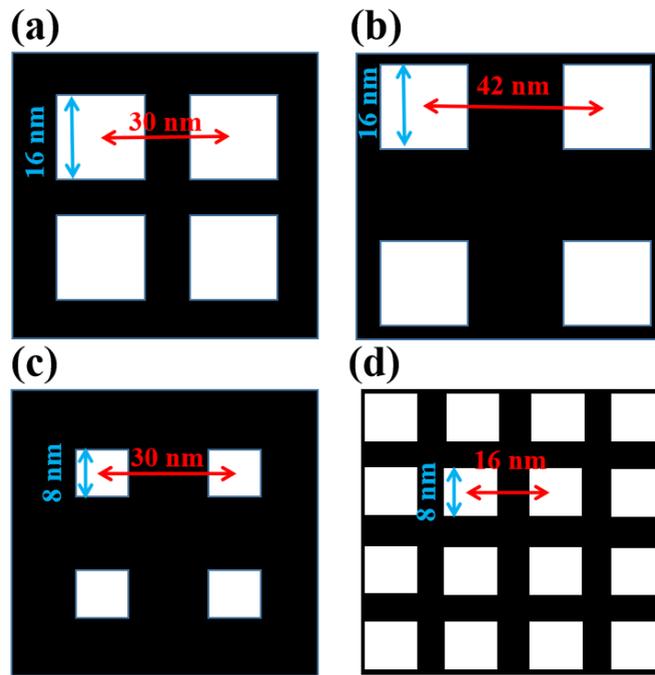
Fig. 1 We are investigating antidotted graphene Samples 1-4 as illustrated in (a)-(d). The radii of the square pores are 8, 8, 4, and 4 nm, respectively, and the corresponding interporous distances are 30, 42, 30, and 16 nm.
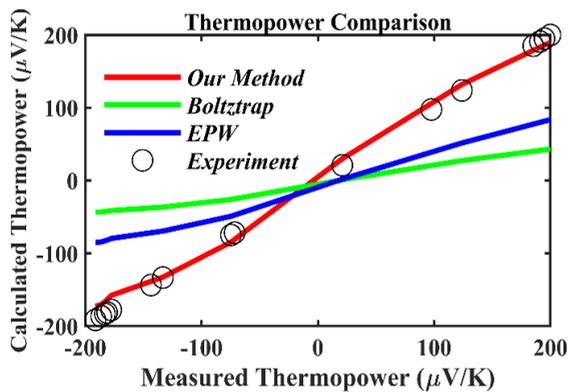

Fig. 2 Comparison of the thermopower of Sample 1 at the room temperature of $T = 300$ K, calculated by our method, the *BoltzTrap* method, and the *EPW* method, with respect to the data measured from the experiment by Xu *et al.*[30]
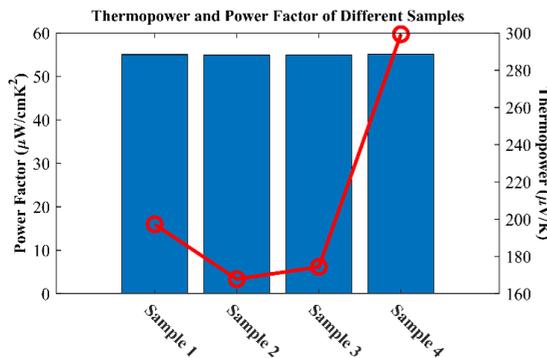

Fig. 3 The thermopower of the four samples differ from each other because they have different pore-radii and/or interporous distances. However, the thermal power factors do not differ from sample to sample, noticeably, which implies easy quality control and inexpensive manufacturing for industrialization.

Therefore, the mini-band gap is negatively correlated with the interporous distance and positively correlated with the pore-radius. However, it is interesting to observe that the power factor does not change significantly from sample to sample. This is suggesting that the cooling or the refrigeration performance of an antidotted graphene is not very sensitive to the distribution variance of either the pore-radius or the interporous distance. This trend is positive news for the quality control of products in large-scale industrialization, which implies a potential for inexpensive manufacturing. We now study the active rates of thermoelectric refrigeration and cooling, respectively. Since the four antidotted graphene samples have almost the same power factor at the optimized condition, we will just illustrate the results for Sample 1 as an instance. Fig. 4 shows the data of the active rates for refrigeration and cooling using Sample 1 when the mid-point temperature is at room temperature. As we can see from the figure, the active rate for cooing is slightly higher than the refrigeration, but generally not noticeably different. The comparison between the optimized and the unoptimized active rates are indicating an advantage of the low-dimensional materials tuned with gate voltage for microscale heat management. When thermoelectric refrigeration or cooling devices are designed, it is preferred that the *p*-leg and the *n*-leg have as similar performance as possible. However, as in the cases of most Peltier materials systems, the performance of the p-type regime is different from the n-type region. The hole-electron asymmetry ratio between the highest achievable active refrigeration/cooling rates for Sample 1 is ~1.17 at room temperature. However, as in most carbon nanomaterials systems, this asymmetry ratio is generally smaller than the
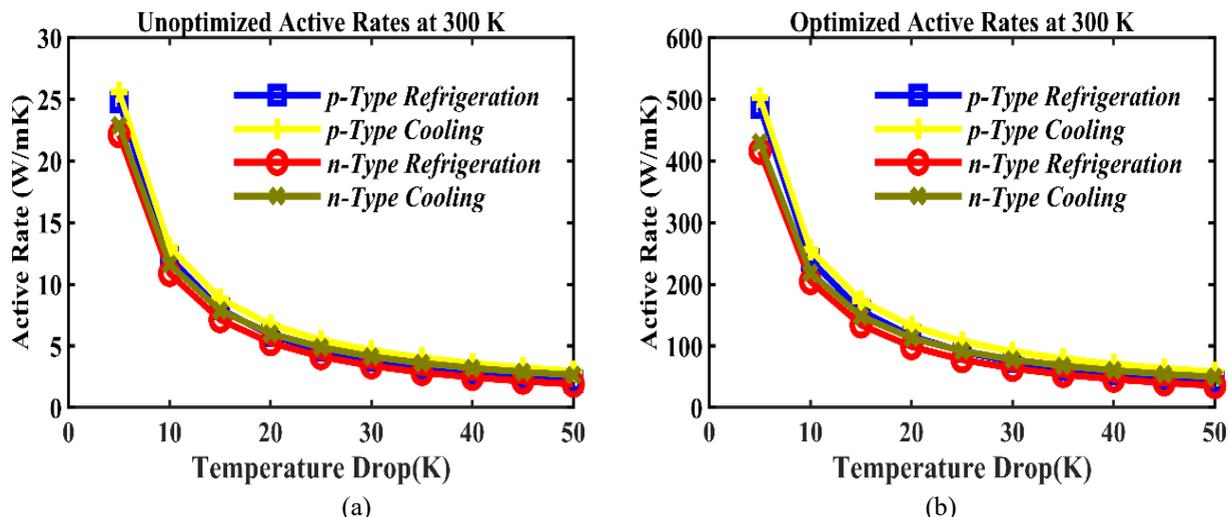
Fig. 4 (a) Unoptimized and the (b) optimized active solid-state refrigeration and cooling out of the Peltier effect by Sample 1, for both the *p*-type and the *n*-type regimes. The mid-point temperature for all the data points is set at T_{mid} = 300 K. The temperature drop marks the difference between the hot side and the cold side, *i.e.* $\Delta T = T_H - T_C$.

values in other commonly used large-*ZT* thermoelectric materials *e.g.* PbTe (8.79)[55] and BaSnO$_3$ (5.32×10^3),[56] which further implies a promising potential for the ultimate manufacturing of Peltier refrigerators and coolers based on the antidotted graphene samples.

As in other carbon systems, the smaller the temperature drop is adopted, the higher performance is expected. When the temperature drop is 10 K, the active refrigeration and cooling rate can possibly achieve as high as ~400 W/mk, which is similar to the thermal conductivity of copper.[57] When the temperature drop is widened, the active rate is generally declining. However, the refrigeration or cooling systems in practice are usually cascaded into different small-range temperature windows to ensure overall performance. Further, we have studied the active rates for Peltier refrigeration and cooling at a cryogenic temperature of 82 K. The data for unoptimized cases and optimized cases are shown

in Figs. 5(a) and (b), respectively. Heat management at this temperature is generally more difficult, and the active rates are significantly smaller compared with the cases at room temperature. However, the highest achievable refrigeration and cooling rates can be ~300 times improved compared to the unoptimized value shown in Fig. 5(a). When we compare the cases of the four different samples, we can see that the performance is still not sensitive to the distribution variance of pore-radius and the interporous distance, which again is helpful for industrialization and inexpensive manufacturing.

4. Conclusions

In conclusion, we have studied the optimized performance of antidotted graphene samples for the potential application in heat management of microelectronics. The active rate for refrigeration and cooling at the room temperature of 300 K and the cryogenic temperature of 82 K are investigated. We have
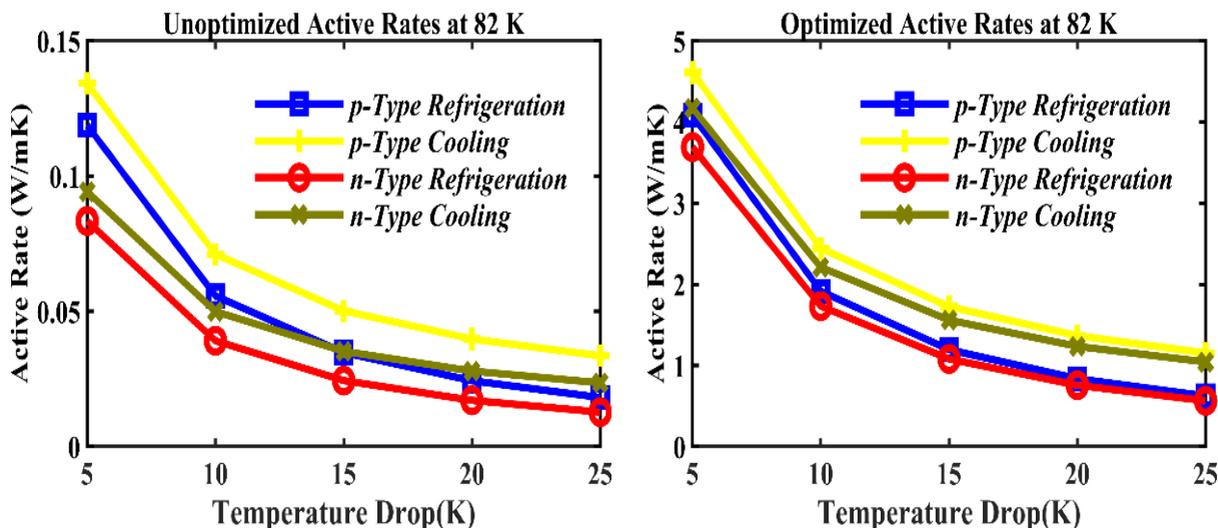

Fig. 5 (a) Unoptimized and the (b) optimized active solid-state refrigeration and cooling out of the Peltier effect by Sample 1, for both the *p*-type and the *n*-type regimes. The mid-point temperature for all the data points is set at T_{mid} = 82 K. The temperature drop marks the difference between the hot side and the cold side, *i.e.* $\Delta T = T_H - T_C$.

found that, by considering the sensitivity of transport to carrier energy, the calculation of thermopower and thermal power factor can be more consistent with the experimental data, compared to the traditional methodologies including the *BoltzTrap* method and the *EPW* method. It is also interesting to see that though the pore-radius and the interpore distance can affect the thermopower, the optimal power factor and the active rates of cooling and refrigeration are, however, very robust against such variations that may be introduced during industry-scale manufacturing. The same methodology can also be used in other layered nanomaterials such as MoS_2, WS_2, $MoSe_2$, WSe_2, blue phosphorene, and tellurene.

Acknowledge

Conflict of Interest

There is no conflict of interest.

Supporting Information

Not applicable.

References

[1] S. K. Moore, *IEEE Spectrum*, 2019, **56**, 8-9, doi: 10.1109/mspec.2019.8847577.

[2] W. Kong, H. Kum, S.-H. Bae, J. Shim, H. Kim, L. Kong, Y. Meng, K. Wang, C. Kim, J. Kim, *Nature Nanotechnology*, 2019, **14**, 927-938, doi: 10.1038/s41565-019-0555-2.

[3] Z. Wu, J. Hao, *Npj 2D Materials and Applications*, 2020, **4**, 4, doi: 10.1038/s41699-020-0139-x.

[4] Y. Liu, X. Duan, H.-J. Shin, S. Park, Y. Huang, X. Duan, *Nature*, 2021, **591**, 43-53, doi: 10.1038/s41586-021-03339-z.

[5] A. Chaves, J. G. Azadani, H. Alsalman, D. R. da Costa, R. Frisenda, A. J. Chaves, S. H. Song, Y. D. Kim, D. He, J. Zhou, A. Castellanos-Gomez, F. M. Peeters, Z. Liu, C. L. Hinkle, S.-H. Oh, P. D. Ye, S. J. Koester, Y. H. Lee, P. Avouris, X. Wang, T. Low, *Nature*, 2020, **4**, 29, doi: 10.1038/s41699-020-00162-4.

[6] A. J. Mannix, Z. Zhang, N. P. Guisinger, B. I. Yakobson, M. C. Hersam, *Nature Nanotechnology*, 2018, **13**, 444-450, doi: 10.1038/s41565-018-0157-4.

[7] J. Mao, G. Chen, Z. Ren, *Nature Materials*, 2021, **20**, 454-461, doi: 10.1038/s41563-020-00852-w.

[8] S. Tang, M. S. Dresselhaus, *Nano Letters*, 2012, **12**, 2021-2026, doi: 10.1021/nl300064d.

[9] S. Tang, M. S. Dresselhaus, *Physical Review B*, 2012, **86**, 075436, doi: 10.1103/physrevb.86.075436.

[10] S. Tang, M. S. Dresselhaus, *Journal of Material Chemistry C*, 2014, **2**, 4710-4726, doi: 10.1039/c4tc00146j.

[11] I. Donmez Noyan, G. Gadea, M. Salleras, M. Pacios, C. Calaza, A. Stranz, M. Dolcet, A. Morata, A. Tarancon, L. Fonseca, *Nano Energy*, 2019, **57**, 492-499, doi: 10.1016/j.nanoen.2018.12.050.

[12] G. Schierning, *Physica Status Solidi (a)*, 2014, **211**, 1235-1249, doi: 10.1002/pssa.201300408.

[13] J. P. Heremans, V. Jovovic, E. S. Toberer, A. Saramat, K. Kurosaki, A. Charoenphakdee, S. Yamanaka, G. J. Snyder, *Science*, 2008, **321**, 554-557, doi: 10.1126/science.1159725.

[14] S. Liu, Y. Qin, B. Qin, Y. Xiao, L.-D. Zhao, *ACS Applied Energy Materials*, 2021, **4**, 11813-11818, doi: 10.1021/acsaem.1c02589.

[15] D. Zhao, G. Tan, *Applied Thermal Engineering*, 2014, **66**, 15-24, doi: 10.1016/j.applthermaleng.2014.01.074.

[16] N. Wang, H.-W. Li, C. Ding, L.-Y. Shi, H.-Z. Jia, Z.-D. Ren, Z.-Y. Zhao, *IEEE Transactions on Electron Devices*, 2018, **65**, 1185-1191, doi: 10.1109/ted.2017.2788899.

[17] J. Duan, X. Wang, X. Lai, G. Li, K. Watanabe, T. Taniguchi, M. Zebarjadi, E. Y. Andrei, *Proceedings of the National Academy of Sciences of the United States of America*, 2016, **113**, 14272-14276, doi: 10.1073/pnas.1615913113.

[18] A. Harzheim, J. Spiece, C. Evangeli, E. McCann, V. Falko, Y. Sheng, J. H. Warner, G. A. D. Briggs, J. A. Mol, P. Gehring, O. V. Kolosov, *Nano Letters*, 2018, **18**, 7719-7725, doi: 10.1021/acs.nanolett.8b03406.

[19] T. G. Pedersen, C. Flindt, J. Pedersen, N. A. Mortensen, A.-P. Jauho, K. Pedersen, *Physical Review Letters*, 2008, **100**, 136804, doi: 10.1103/physrevlett.100.136804.

[20] S. Heydrich, M. Hirmer, C. Preis, T. Korn, J. Eroms, D. Weiss, C. Schüller, *Applied Physics Letters*, 2010, **97**, 043113, doi: 10.1063/1.3474613.

[21] X. Wan, D. Ma, D. Pan, L. Yang, N. Yang, *Materials Today Physics*, 2021, **20**, 100445, doi: 10.1016/j.mtphys.2021.100445.

[22] S. Hu, S. An, N. Yang, B. Li, *Small*, 2017, **13**, 1602726, doi: 10.1002/smll.201602726.

[23] H. Ding, G. Peng, S. Mo, D. Ma, S. W. Sharshir, N. Yang, *Nanoscale*, 2017, **9**, 19066-19072, doi: 10.1039/c7nr05304e.

[24] C. Tang, X. Yu, G. Li, N. Yang, J. Lü, *ES Materials & Manufacturing*, 2018, **3**, 16-21, doi: 10.30919/esmm5f203.

[25] Z. Luo, N. J. Pinto, Y. Davila, A. T. Charlie Johnson, *Applied Physics Letters*, 2012, **100**, 253108, doi: 10.1063/1.4729828.

[26] Y. Ye, L. Gan, L. Dai, Y. Dai, X. Guo, H. Meng, B. Yu, Z. Shi, K. Shang, G. Qin, *Nanoscale*, 2011, **3**, 1477, doi: 10.1039/c0nr00999g.

[27] O. Lehtinen, J. Kotakoski, A. V. Krasheninnikov, J. Keinonen, *Nanotechnology*, 2011, **22**, 175306, doi: 10.1088/0957-4484/22/17/175306.

[28] C.-L. Wu, H.-T. Lin, H.-A. Chen, S.-Y. Lin, M.-H. Shih, C.-W. Pao, *Materials Today Communications*, 2018, **17**, 60-68, doi: 10.1016/j.mtcomm.2018.08.006.

[29] L. Z. Liu, S. B. Tian, Y. Z. Long, W. X. Li, H. F. Yang, J. J. Li, C. Z. Gu, *Vacuum*, 2014, **105**, 21-25, doi: 10.1016/j.vacuum.2014.01.015.

[30] D. Xu, S. Tang, X. Du, Q. Hao, *Carbon*, 2019, **144**, 601-607, doi: 10.1016/j.carbon.2018.12.080.

[31] G. K. H. Madsen, D. J. Singh, *Computer Physics Communications*, 2006, **175**, 67-71, doi: 10.1016/j.cpc.2006.03.007.

[32] J. Noffsinger, F. Giustino, B. D. Malone, C.-H. Park, S. G. Louie, M. L. Cohen, *Computer Physics Communications*, 2010, **181**, 2140-2148, doi: 10.1016/j.cpc.2010.08.027.

[33] S. Tang, T. Cai, G. M. Wang, J. G. Liang, X. Li, J. Yu, *Scientific Report*, 2018, **8**, 6422, doi: 10.1038/s41598-018-24929-4.

[34] S. Tang, *ES Materials & Manufacturing*, 2019, 4, 45-50, doi: 10.30919/esmm5f213.

[35] D. Rode, *Physical Review B*, 1970, **2**, 1012, doi: 10.1103/PhysRevB.2.1012.

[36] N. Miller, E. E. Haller, G. Koblmüller, C. Gallinat, J. S. Speck, W. J. Schaff, M. E. Hawkridge, K. Man Yu, J. W. Ager, *Physical Review B*, 2011, **84**, 075315, doi: 10.1103/PhysRevB.84.075315.

[37] G. Ng, D. Vasileska, D. K. Schroder, *Journal of Applied Physics*, 2009, **106**, 053719, doi: 10.1063/1.3212532.

[38] A. T. Ramu, L. E. Cassels, N. H. Hackman, H. Lu, J. M. O. Zide, J. E. Bowers, *Journal of Applied Physics*, 2010, **107**, 083707, doi: 10.1063/1.3366712.

[39] A. T. Ramu, J. E. Bowers, *Applied Physics Letters*, 2012, **101**, 173905, doi: 10.1063/1.4764517.

[40] A. Faghaninia, J. W. Ager, C. S. Lo, *Physical Review B*, 2015, **91**, 235123, doi: 10.1103/physrevb.91.235123.

[41] Q. Chen, G. A. Fiete, *Physical Review B*, 2016, 93, 155125, doi: 10.1103/physrevb.93.155125.

[42] B. Z. Rameshti, R. Asgari, *Physical Review B*, 2016, **94**, 205401, doi: 10.1103/physrevb.94.205401.

[43] M. Zare, B. Z. Rameshti, F. G. Ghamsari, R. Asgari, *Physical Review B*, 2017, **95**, 045422, doi: 10.1103/physrevb.95.045422.

[44] D. Kim, R. Du, S.-Y. Yu, Y. Yin, S. Dong, Q. Li, S. E. Mohney, X. Li, S. Tadigadapa, *Nanotechnology*, 2020, **31**, 365703, doi: 10.1088/1361-6528/ab97d2.

[45] T. Ando, H. Matsumura, T. Nakanishi, *Physica B: Condensed Matter*, 2002, **323**, 44-50, doi: 10.1016/s0921-4526(02)00964-x.

[46] H. J. Li, W. G. Lu, J. J. Li, X. D. Bai, C. Z. Gu, *Physical Review Letters*, 2005, **95**, 086601, doi: 10.1103/physrevlett.95.086601.

[47] P. Poncharal, C. Berger, Y. Yi, Z. L. Wang, W. A. de Heer, *The Journal of Physical Chemistry B*, 2002, **106**, 12104-12118, doi: 10.1021/jp021271u.

[48] Z. Wu, Y. Xing, W. Ren, Y. Wang, H. Guo, *Carbon*, 2019, **149**, 364-369, doi: 10.1016/j.carbon.2019.04.062.

[49] Y. Zhu, C. Chen, S. Wu, R. Cheng, L. Cheng, W.-L. Zhou, *Journal of Applied Physics*, 2020, **128**, 064302, doi: 10.1063/5.0009406.

[50] P. Gehring, J. M. Thijssen, H. S. J. van der Zant, *Nature Reviews Physics*, 2019, **1**, 381-396, doi: 10.1038/s42254-019-0055-1.

[51] C. Maier, T. Brydges, P. Jurcevic, N. Trautmann, C. Hempel, B. P. Lanyon, P. Hauke, R. Blatt, C. F. Roos, *Physical Review Letters*, 2019, **122**, 050501, doi: 10.1103/physrevlett.122.050501.

[52] H. Zhang, D. E. Liu, M. Wimmer, L. P. Kouwenhoven, *Nature Communication*, 122019, **10**, 1-7.

[53] S. Wang, B.-C. Lin, A.-Q. Wang, D.-P. Yu, Z.-M. Liao, *Advances in Physics: X*, 2017, **2**, 518-544, doi: 10.1080/23746149.2017.1327329.

[54] M. Zebarjadi, *Applied Physics Letters*, 2015, **106**, 203506, doi: 10.1063/1.4921457.

[55] L. Xu, Y. Zheng, J.-C. Zheng, *Physical Review B*, 2010, **82**, 195102, doi: 10.1103/physrevb.82.195102.

[56] J. Li, Z. Ma, R. Sa, K. Wu, *RSC Advances*, 2017, **7**, 32703-32709, doi: 10.1039/c7ra05193j.

[57] R. B. Bird, *Applied Mechanics Review*, 2002, **55**, R1-R4, doi: 10.1115/1.1424298.

Author Information

Dr. Shuang Tang *joined the State University of New York Polytechnic Institute as a faculty member in 2015, after he received his PhD in Materials Science and Engineering from the Massachusetts Institute of Technology, advised by Institute Professor Mildred Dresselhaus. His research interests include developing new materials systems based on nanoscience and nanotechnology for the application of sustainable energy, heat management, information technology, computer chips and satellite parts, and developing modern methods for doctoral, graduate and undergraduate education of science and engineering.*

Mr. Andy Juan *is now a student at SUNY Poly majored in Mechanical Engineering. His research focuses on condensed matter physics and materials science, especially the application in sustainable energy and nuclear engineering.*

Mr. David Drysdale *is a current senior at SUNY Poly with a major of mechanical engineering and a minor of Math. His research interests include materials science and water mining on Mars.*

Mr. Joseph Duarte Menjivar *is now an undergraduate student at the SUNY Poly. He is now focusing on developing atomistic simulation for the application of solid state electricity generation.*

Mr. Jason Guzman *is now a mechanical engineering student at the SUNY Poly. His research interests include atomistic modeling of materials science for energy applications.*